

# Comparison of Microinstability Properties for Stellarator Magnetic Geometries\*

G. Rewoldt, L.-P. Ku,  
and W.M. Tang

*Princeton University  
Plasma Physics Laboratory*

With thanks to W. Guttenfelder,  
V. Kornilov, N. Nakajima,  
J. Nuehrenberg, D. Spong,  
J.N. Talmadge, H. Yamada,  
and M. Zarnstorff,  
for providing input data and for  
discussions

\*Work supported by U.S.  
D.O.E. Contract No.  
DE-AC02-76-CHO-3073

# Introduction

- Differing regions of localization of trapped electrons, and of “good” (stabilizing) and “bad” (destabilizing) magnetic curvature, along magnetic field lines, can affect linear growth rates and real frequencies of Ion Temperature Gradient (ITG) modes and Trapped-Electron Modes (TEMs) in tokamaks and stellarators.
- Here, we compare ITG-TEM mode properties for stellarator cases corresponding to different present and planned stellarators, and to corresponding axisymmetric cases.

# Introduction-2

- Use stellarator (non-axisymmetric) version of FULL code, in electrostatic, collisionless limit, on single, chosen magnetic surface. Includes trapped particles, complete FLR (Bessel functions), transit frequency, bounce frequency, and magnetic drift frequency resonances, for all included species, in high- $n$ , radially-local limit (ballooning representation).

# Cases

- LHD
- NCSX (non-zero total current)
- NCSX-J=0 (zero total current)
- Wendelstein 7-X (W7-X)
- HSX
- QPS
- NCSX-SYM (like NCSX, but keep  $n=0$  components only in MHD equilibrium)
- NCSX-TOK (like NCSX-SYM, but change to tokamak-like  $q$  or  $\iota$  profile)
- NCSX-BETA (like NCSX, but with 4% volume-average  $\beta$ )

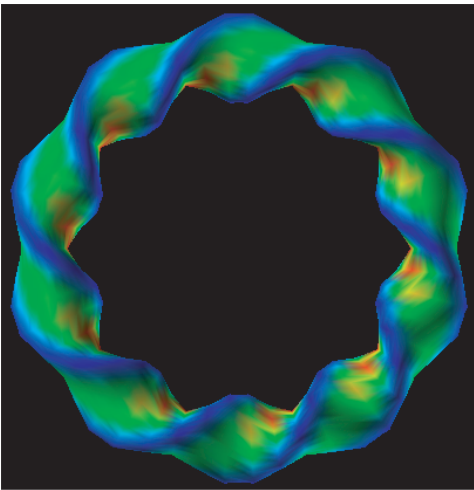
# Cases-2

- All cases have same geometric-center major radius
- All cases have same  $B_0$  at geometric center
- All cases have same density and temperature profile shapes, and thus pressure profile shape (taken from LHD inward-shifted experimental shot), but with very low volume-average  $\beta = 0.1\%$  (except for NCSX-BETA case)

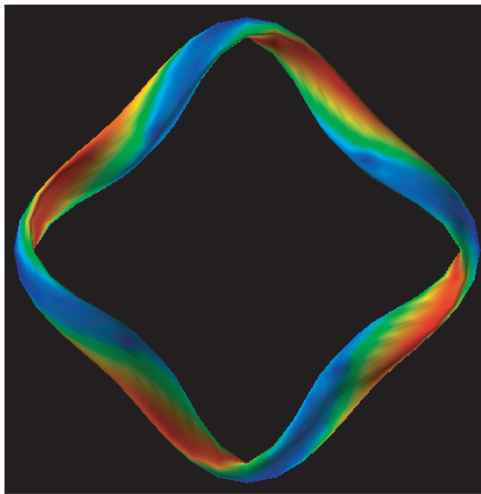
# Cases-3

- Shapes of last closed flux surfaces shown in Fig. 1, with magnetic field strength indicated (red=strongest, blue=weakest)
- Rotational transform  $\iota$  profiles shown in Fig. 2
- MHD equilibrium from VMEC, with results processed through TERPSICHORE and VVBAL

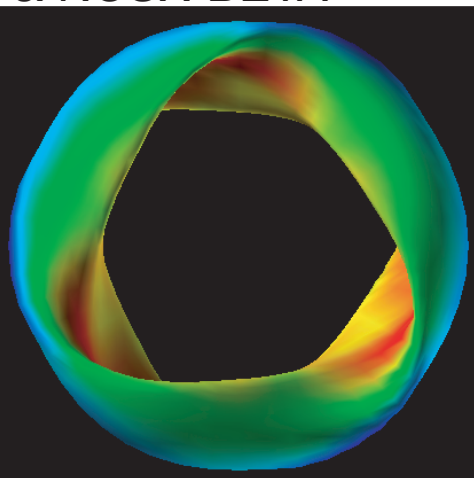
LHD



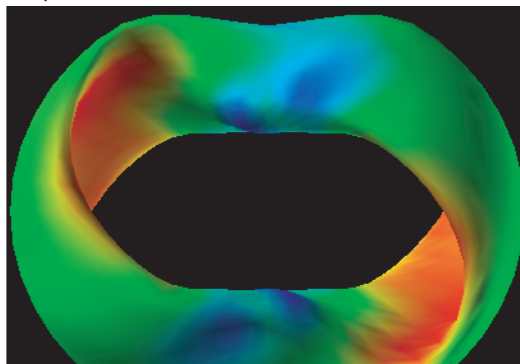
HSX



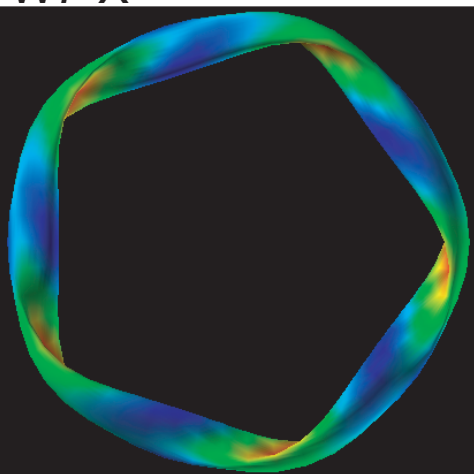
NCSX & NCSX-J=0  
& NCSX-BETA



QPS



W7-X



NCSX-SYM  
& NCSX-TOK

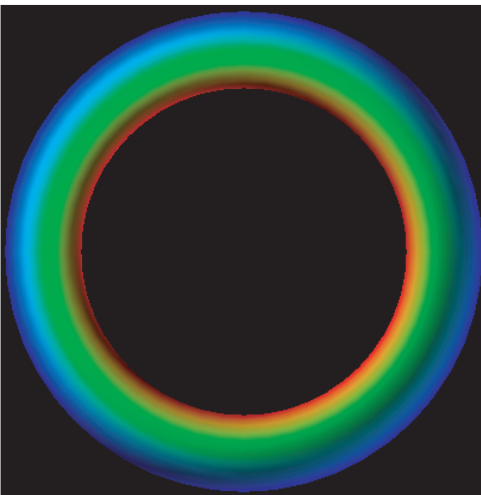


Fig. 1

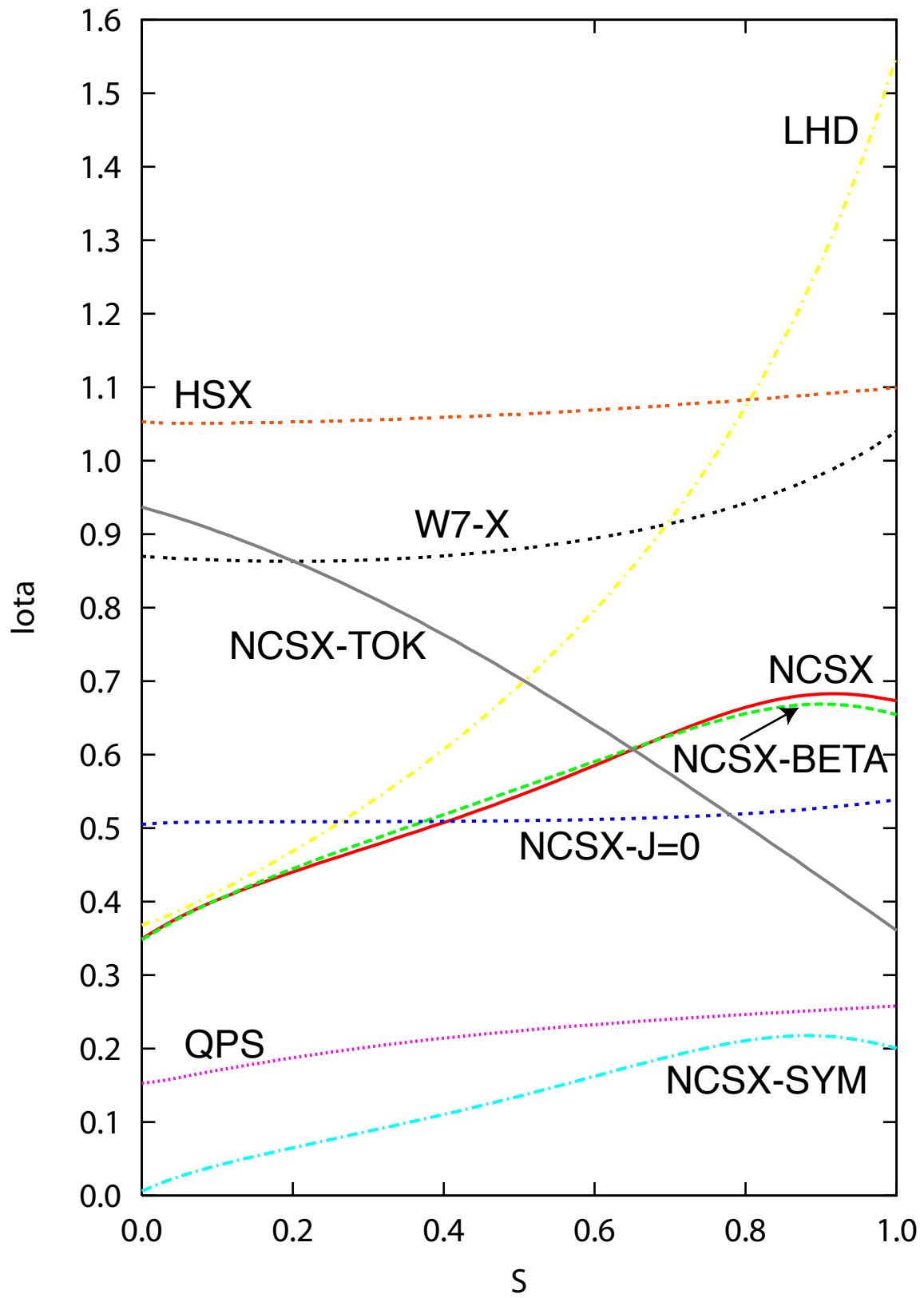


Fig. 2

# Results

- All calculations for magnetic surface with  $s = 0.74 \propto (r/a)^2$ , with  $n_i = n_e$  and  $T_i = T_e$  (include electrons & deuterium only)
- Start with  $\alpha = \zeta - q\theta = 0$ ,  $\theta_0 (= \theta_k) = 0$ ,  $\eta = \eta_i = \eta_e = 2.66$  (LHD experimental value), and  $k_{\perp}(\theta = 0)$   
 $\rho_i = 0.30$ , with  $\eta_j = d \ln T_j / d \ln n_j$
- ITG mode and TEM mode “hybridize” to form single ITG-TEM root!
- First, maximize linear growth rate  $\gamma$  over  $\alpha$  (gives  $\alpha^{\text{Max}}$  for each case)
- Second, maximize linear growth rate  $\gamma$  over  $\theta_0$  (gives  $\theta_0^{\text{Max}}$  for each case) for  $\alpha = \alpha^{\text{Max}}$

# Results-2

- Third, maximize linear growth rate  $\gamma$  over  $k_{\perp}(\theta=0)\rho_i$  (gives  $k_{\perp}^{\text{Max}}(\theta=0)\rho_i$  for each case) for  $\alpha = \alpha^{\text{Max}}$  and  $\theta_0 = \theta_0^{\text{Max}}$
- Finally, vary  $\eta = \eta_i = \eta_e$  for  $\alpha = \alpha^{\text{Max}}$  and  $\theta_0 = \theta_0^{\text{Max}}$  and  $k_{\perp}(\theta=0)\rho_i = k_{\perp}^{\text{Max}}(\theta=0)\rho_i$
- Magnetic field strength variation along field line (in ballooning representation) for  $\alpha = \alpha^{\text{Max}}$  and  $\theta_0 = \theta_0^{\text{Max}}$  shown for nine cases in Fig. 3, with illustrative trapped-particle orbit extents
- Corresponding variation of  $k_{\perp}^2(\theta)/n^2$  shown in Fig. 4
- Corresponding variation of curvature function  $\mathbf{k}_{\perp} \cdot \{\mathbf{b} \times [(\mathbf{b} \cdot \nabla) \mathbf{b}]\} / n$  (where  $\mathbf{b} = \mathbf{B}/B$ ) shown in Fig. 5

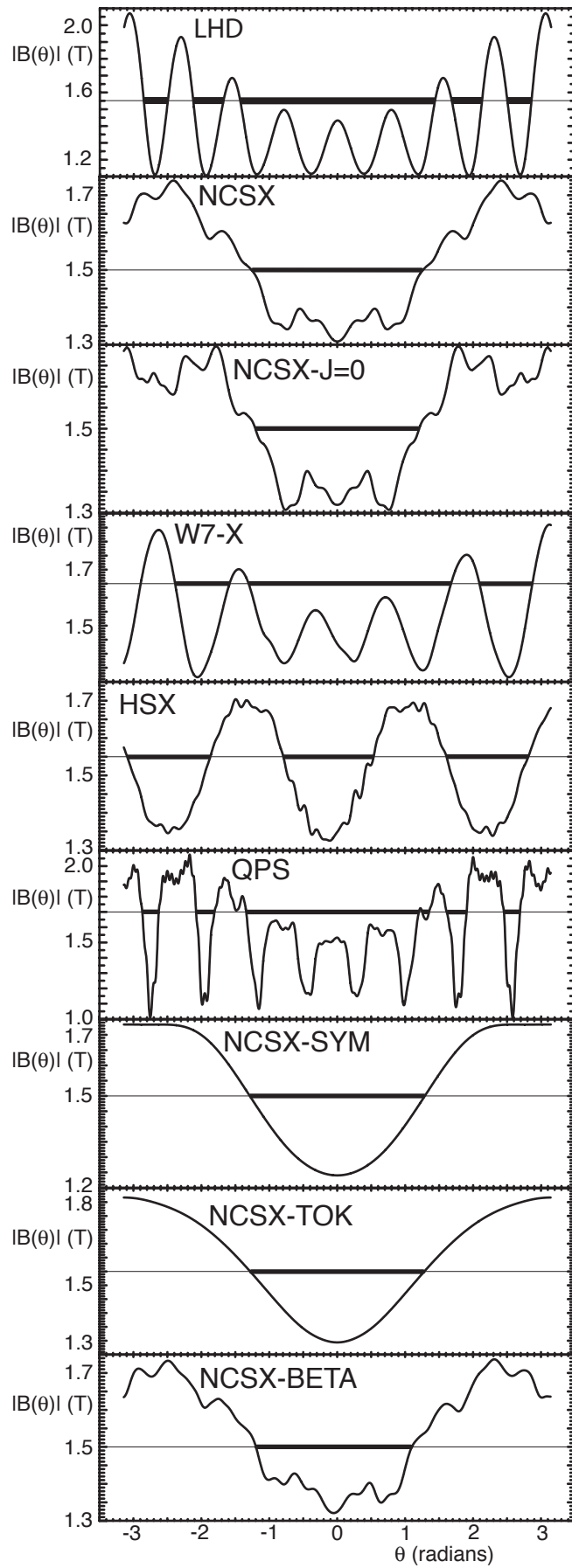


Fig. 3

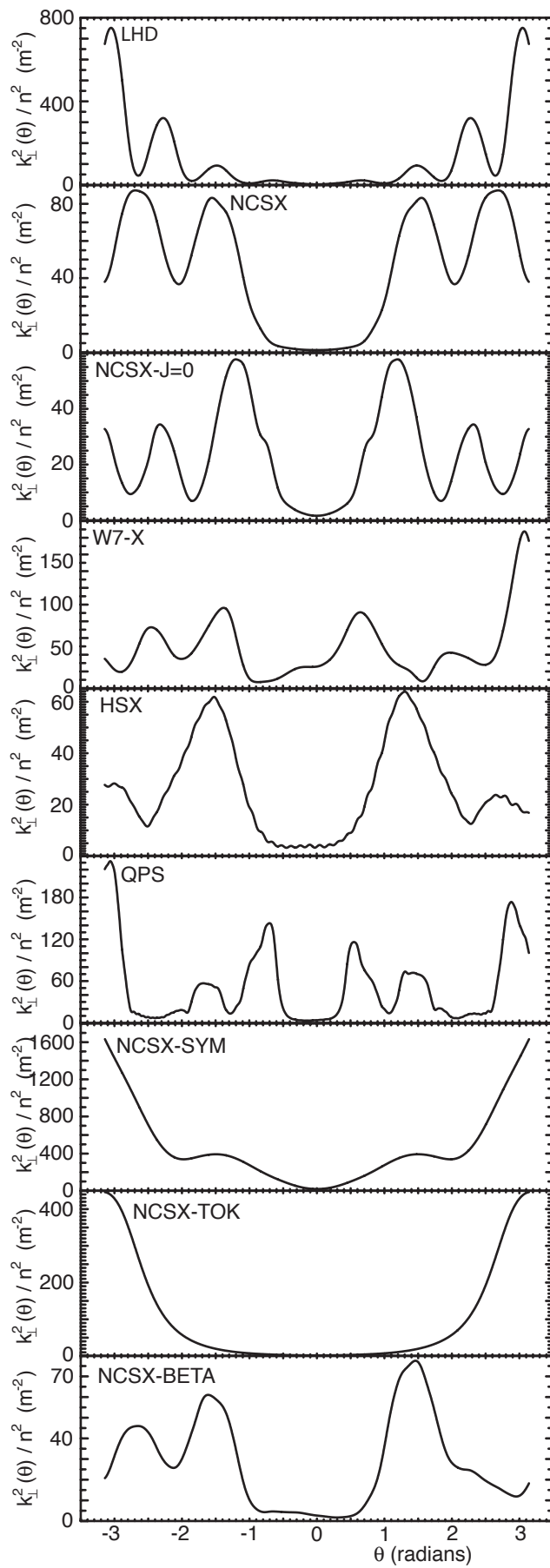


Fig. 4

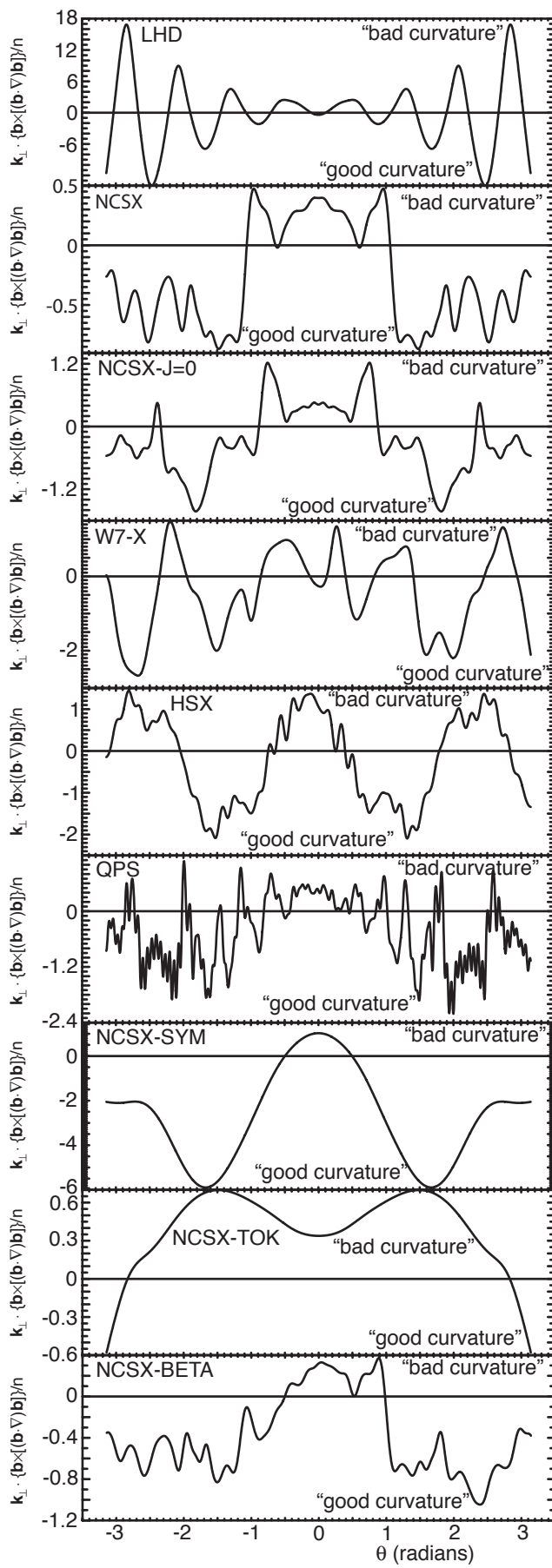


Fig. 5

# Results-3

- Variation of growth rate  $\gamma$  and real frequency  $\omega_r$  with  $M\alpha$  (where  $M$  = number of periods) for starting values for nine cases shown in Fig. 6
- Corresponding variation of  $\gamma$  and  $\omega_r$  with  $\theta_0$  (for  $\alpha = \alpha^{\text{Max}}$  and other starting values) shown in Fig. 7
- Corresponding variation of  $\gamma$  and  $\omega_r$  with  $k_{\perp}(\theta=0)\rho_i$  (for  $\alpha = \alpha^{\text{Max}}$  and  $\theta_0 = \theta_0^{\text{Max}}$  and other starting values) shown in Fig. 8
- Linear eigenfunctions along field line (in ballooning representation) (for  $\alpha = \alpha^{\text{Max}}$  and  $\theta_0 = \theta_0^{\text{Max}}$  and  $k_{\perp}(\theta=0)\rho_i = k_{\perp}^{\text{Max}}(\theta=0)\rho_i$ ) shown in Fig. 9

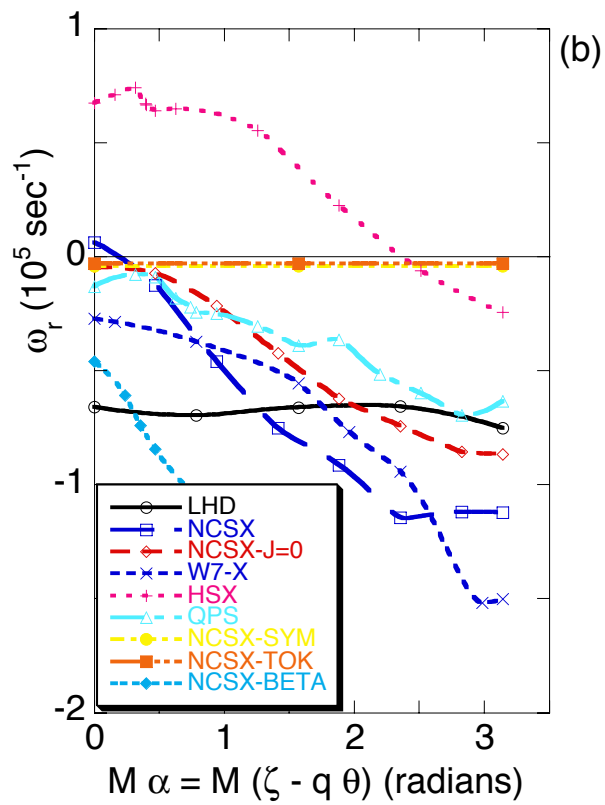
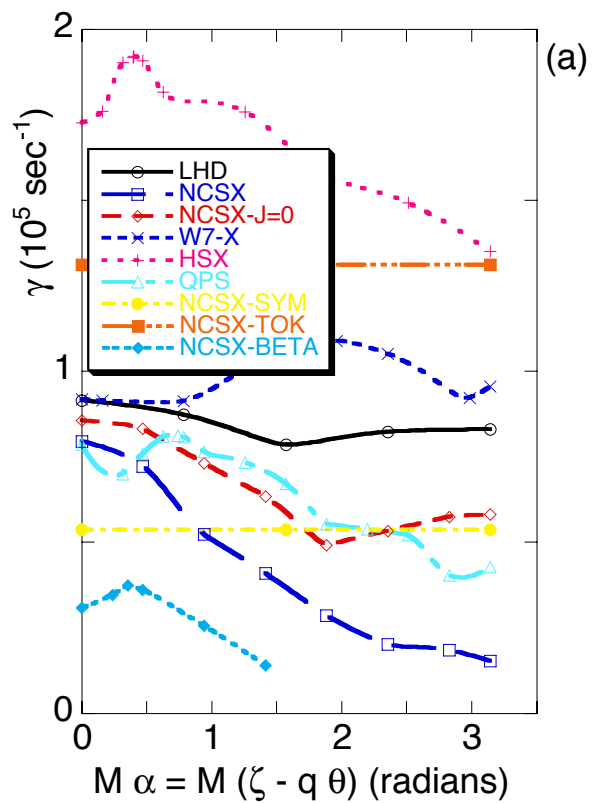


Fig. 6

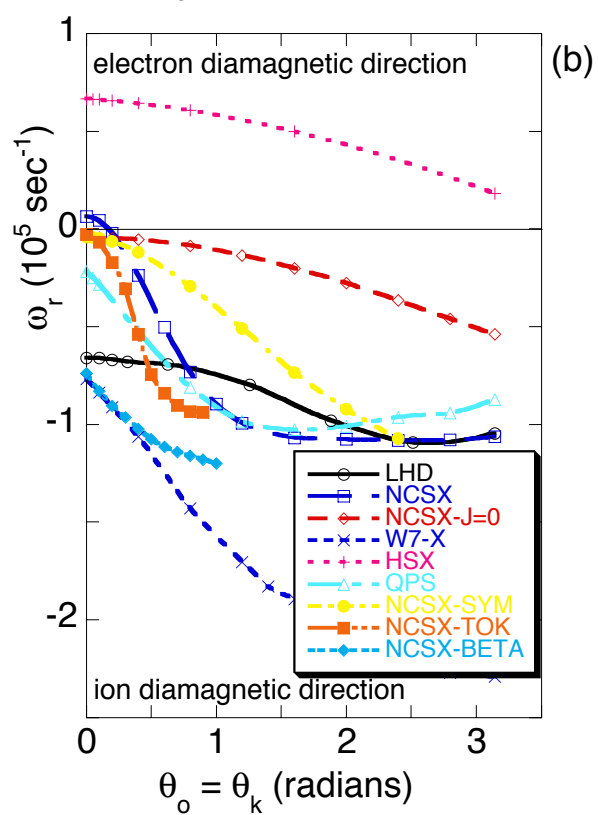
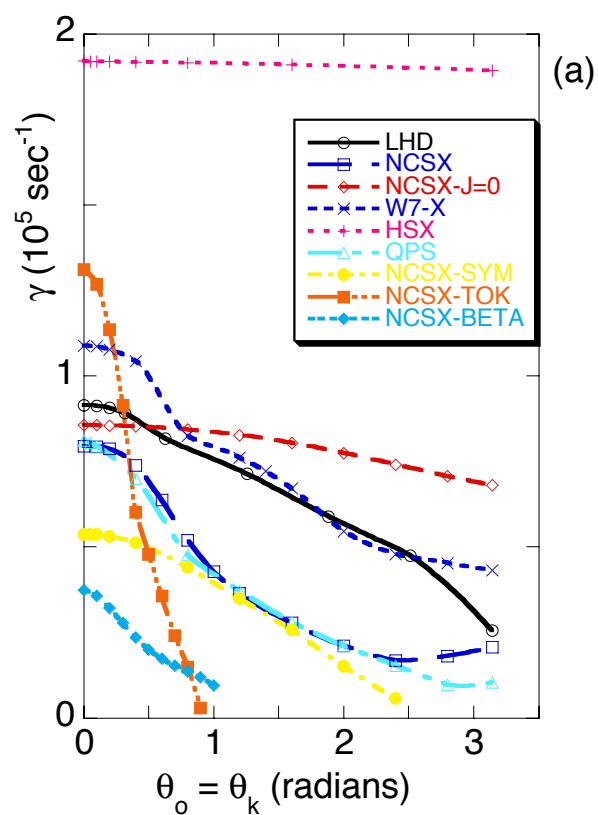


Fig. 7

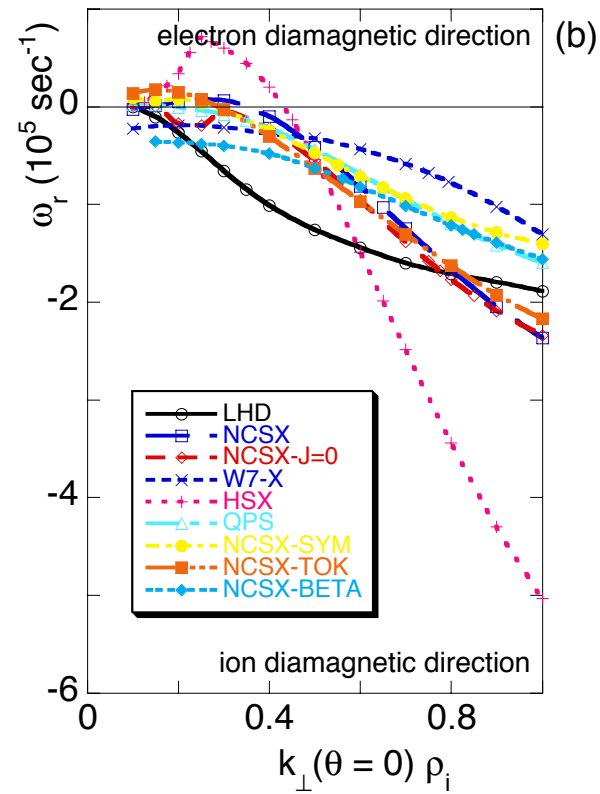
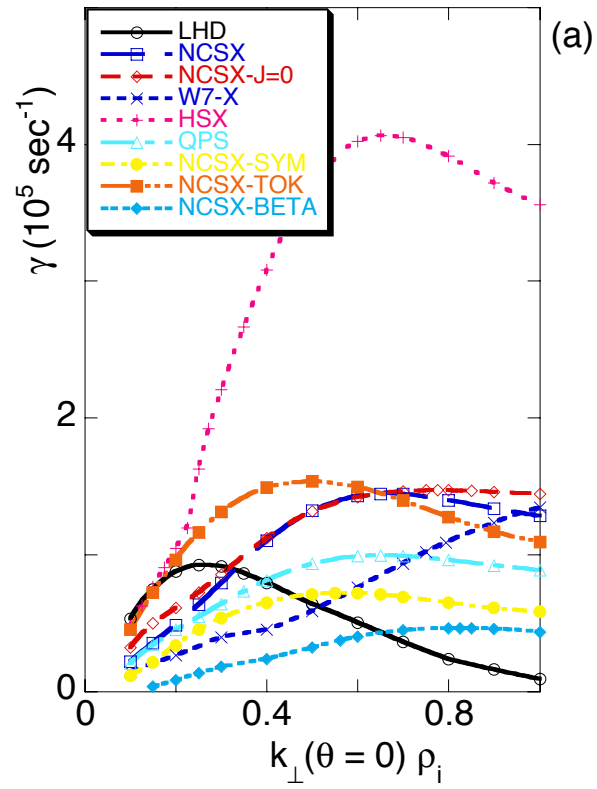


Fig. 8

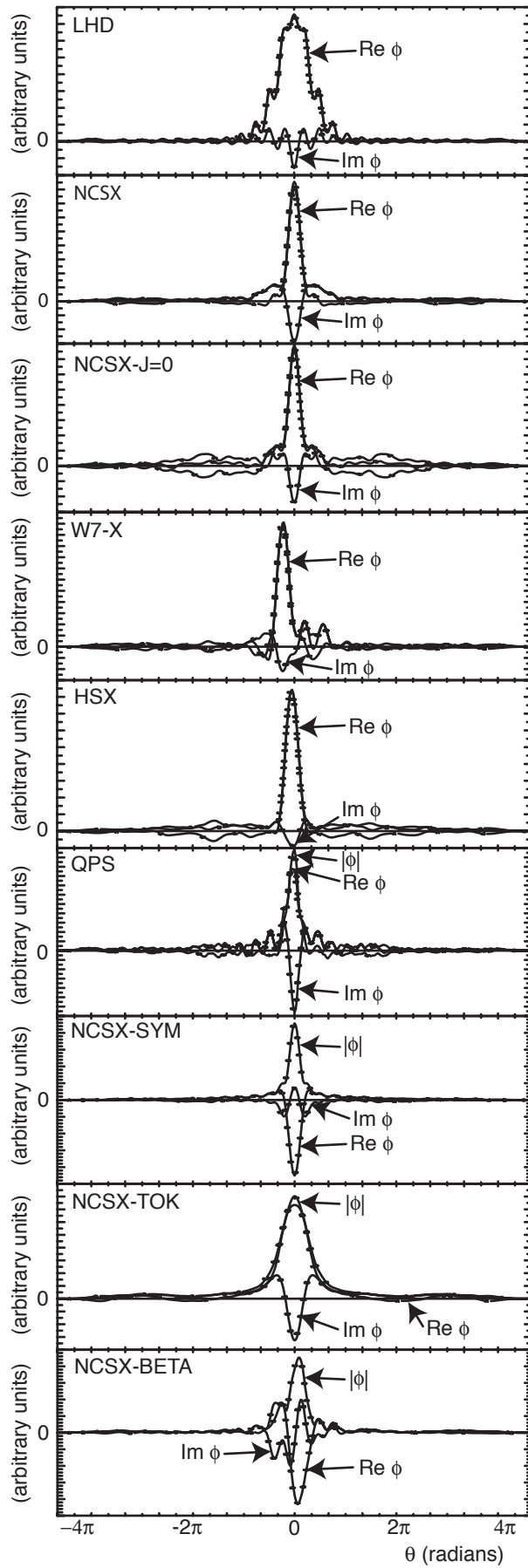


Fig. 9

# Results-4

- Variation of  $\gamma$  and  $\omega_r$  with  $\eta = \eta_i = \eta_e$  (for  $\alpha = \alpha^{\text{Max}}$  and  $\theta_0 = \theta_0^{\text{Max}}$  and  $k_{\perp}(\theta=0)\rho_i = k_{\perp}^{\text{Max}}(\theta=0)\rho_i$ ) shown in Fig. 10
- ITG destabilization mechanism (non-resonant) dominant at large  $\eta_i$  - strongly unstable for all cases
- Collisionless TEM destabilization mechanism (resonant with orbit-average magnetic drift frequency) dominant for small  $\eta_i$  - strongly unstable for some cases and weakly unstable or stable for other cases
- Small- $\eta_i$  result depends on details of localization of trapped electrons and of localization of good and bad curvature!

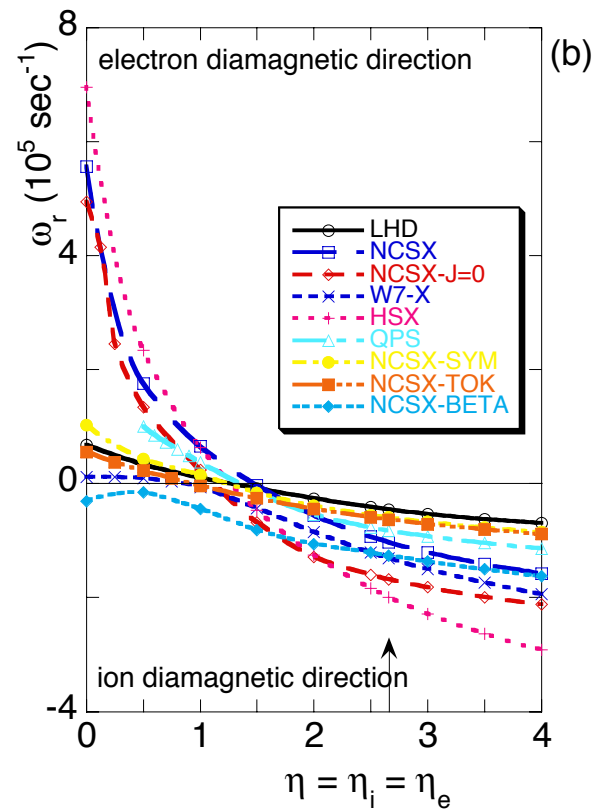
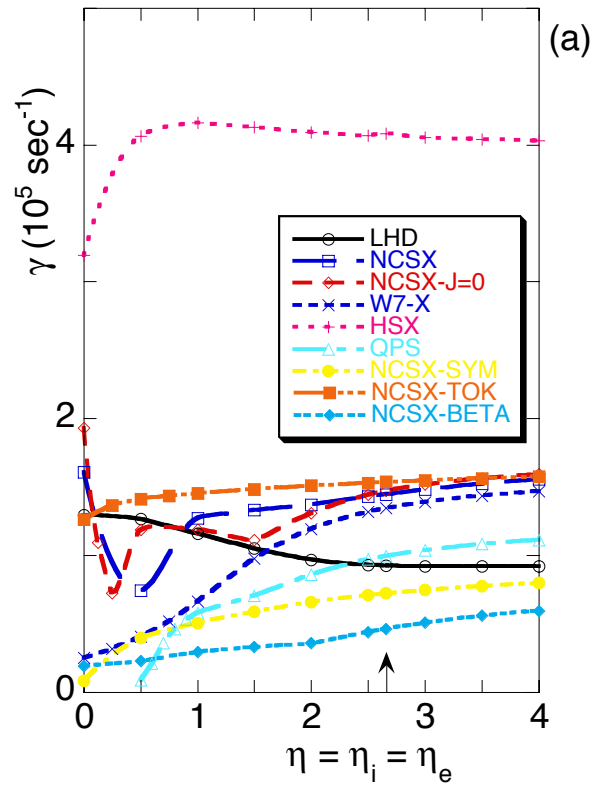


Fig. 10

# Conclusions

- For NCSX, NCSX-J=0, and LHD cases,  $\gamma$  rises as  $\eta$  approaches zero, indicating rather strong destabilization from trapped-electron magnetic drifts (bad curvature)
- For W7-X, NCSX-SYM, and NCSX-BETA cases,  $\gamma$  falls as  $\eta$  approaches zero, indicating weak trapped-electron destabilization. For HSX and NCSX-TOK cases,  $\gamma$  also falls as  $\eta$  approaches zero, but overall destabilization is larger
- For QPS case,  $\gamma$  also falls as  $\eta$  approaches zero, and ITG-TEM mode is completely stable for  $\eta < 0.5!$

# Conclusions-2

- NCSX-SYM case, with negative magnetic shear (in tokamak sense) less unstable than NCSX-TOK case, with positive shear, as expected
- NCSX-BETA case (with large volume-average  $\beta$ ) less unstable than NCSX case, (with almost zero  $\beta$ ), showing Shafranov-shift-like reduction in trapped-electron bad curvature!
- For all of these magnetic geometries, this ITG-TEM mode is strongly unstable linearly if the temperature gradient is large!